

Zernike's feature descriptors for Iris Recognition with SVM

Juan Reyes-López, Sergio Campos and Héctor Allende

Departamento de Informática

Universidad Técnica Federico Santa María, UTFSM

Valparaíso, Chile

Email: jareyes@hpc.cl; scampos@inf.utfsm.cl; hallende@inf.utfsm.cl

Rodrigo Salas

Departamento de Ingeniería Biomédica

Universidad de Valparaíso, UV

Valparaíso, Chile

Email: rodrigo.salas@uv.cl

Abstract—Valuable information of the iris is intrinsically located in its natural texture, therefore preserve and extract the most relevant features for biometric recognition is of paramount importance. The iris pattern is subject to translation, scaling and rotation, consequently the variations produced by these artifacts must be minimized.

The main contribution of this work consists on performing a comparison between the descriptive power of the Zernike and pseudo Zernike polynomials for the identification of iris images using a Support Vector Machine (SVM) as a classifier.

Experiments with the iris data set obtained from the Bath University repository show that our proposal yields high levels of accuracy.

Keywords—Iris Recognition, Zernike Moments, Pseudo Zernike Moments, Feature extraction, Support Vector Machine

I. INTRODUCTION

The authentication of a person identity in an univocal and automatic way is a requirement by current standards. A fundamental issue in the design of an image pattern recognition system is related to the extraction and selection of the appropriate features from the object. It is desired that these features describe the object in a compact and unambiguous form. Furthermore the features should be invariant with respect to the position, size, and orientation of the object.

The first known algorithm for iris recognition was proposed by Daugman [1]. The Daugman's system consists mainly on the following three major stages: pre-processing, feature extraction and classification. First, the aim of the pre-processing stage is to detect the edges of the pupil and iris and to locate the position of the iris within the image with an integro-differential operator. Then the process continues with the extraction of a pattern of the iris image by methods of feature extraction such as bidimensional Wavelets and, finally, it performs the classification process with the XOR function applied to the iriscodes.

Wildes [2] proposed a variation to the Daugman [3] approach with the following characteristics. The algorithm finds the edges of the pupil and iris in two steps: first the image is converted into a binary edge map and then a Hough transform

is used to detect circles. The feature extraction is performed using Laplacian or Gaussian filter at multiple scales. Finally, the matching or similarity calculation between two iris images is based on normalized correlation between the iris input image and the ones registered in the database.

On the other hand, Sánchez-Reillo et al. [4] used the left and right portion of the iris by applying a polar transformation bounded by the angles covered, thus avoiding to work with the missing data due to eye lashes. In this work, the authors used Gabor filters for feature extraction, which is a very popular among works found in the literature.

Currently, various machine learning algorithms have been employed for iris recognition. For example, Cho et al. [5] presented an algorithm based on LVQ (*Learning Vector Quantization*) to classify patterns extracted by two dimensional Wavelets transform. The V. Neagoe [6] proposal is based on HSOM (a variant of a Self-Organizing Maps that support the Hamming distance) to compute the adjustment of feature patterns.

The Zernike moments [7] have been successfully applied to image analysis and processing (see for example the works of Khotanzad et al. [8] and Arvachet et al. [9]), and recently these orthogonal polynomials have been extended for applications in biometrical systems (see for example the works of Lu et al. [10] and Deepika et al. [11]). An important property of the Zernike moments is that they are invariant to rotation and, moreover, they can be improved to be invariant to scale and translation (see [12] and [13]).

The Pseudo Zernike moments are an improved version of Zernike moments [14] and also have been successfully used as feature extraction method in biometrics systems, they have been used in face recognition (see [15] and [16]), fingerprint verification [17], among others.

In this work, we propose an iris identification system with the following characteristics. The iriscodes are represented by a set of Zernike descriptors in a feature vector, and this information is further used as an input to a Support Vector Machine (SVM) that is builded as a 1 against 1 classifier to identify the user's eye. The method searches within the database for those iris patterns that are the most similar to the user input pattern. The same process was made with the pseudo Zernike descriptor in order to compare both approaches.

¹The work of H. Allende was supported by the research grant Fondecyt 1110854, the work of R. Salas was supported by the research grant DIPUV 37/2008 and the work of S. Campos was supported by the DGIP-UTFSM grant.

In order to test the performance of the proposed methods, a set of eye images obtained from the *Bath University Repository* [18] were used. Figure 1 shows an example of the eye images contained in this database.



Fig. 1. Examples images of the Bath University database.

This work is structured as follows. In section 2, the theoretical framework related to the Zernike moments, pseudo Zernike moments and support vector machine classifier is given. In section 3, the proposed iris recognition system is explained, where the pre-processing, feature extraction and classification stages are given in details. In section 4, experimental results with eye image samples obtained from the *Bath University repository* are exposed to evaluate the performance of the proposed techniques. Finally, in section 5, concluding remarks and future works are given.

II. THEORETICAL FRAMEWORK

A. Zernike Moments

The Zernike polynomials were introduced by F. Zernike in 1934 [19]. The set of Zernike polynomials is formed by complex polynomials that are orthogonal inside the unit circle. The Zernike moments are defined as the projection of the input patterns into the space of the orthogonal basis functions $V_{pq}(x, y)$ known as Zernike polynomials $V_{pq}(x, y) = V_{pq}(r, \theta) = R_{pq}(r)e^{iq\theta}$, where $r = \sqrt{x^2 + y^2}$ is the distance from the origin point $(0, 0)$ to the point (x, y) , $\theta = \arctan(y/x)$ is the angle formed by the x axis and r in anticlockwise, p and q are order and repetition respectively with $p \geq 0$, $|p| \geq q$, $p - |q|$ is even, $i = \sqrt{-1}$. $R_{pq}(r)$ (figure 2) is defined as:

$$R_{pq}(r) = \sum_{s=0}^{\frac{p-|q|}{2}} (-1)^s \cdot \frac{(p-s)!}{s! \cdot \left(\frac{p+|q|}{2} - s\right)! \cdot \left(\frac{p-|q|}{2} - s\right)!} r^{p-2s}$$

The Zernike moment of order p and repetition q for a continuous function $f(x, y)$, with $x^2 + y^2 \leq 1$, is defined as:

$$Z_{pq} = \frac{p+1}{\pi} \int_0^{2\pi} \int_0^1 [V_{pq}(r, \theta)]^* f(r \cos \theta, r \sin \theta) r dr d\theta$$

where $[c]^*$ denotes the complex conjugate of c .

In order to compute the Zernike's moments to a digital image (see [8]), the integrals are discretized as follows:

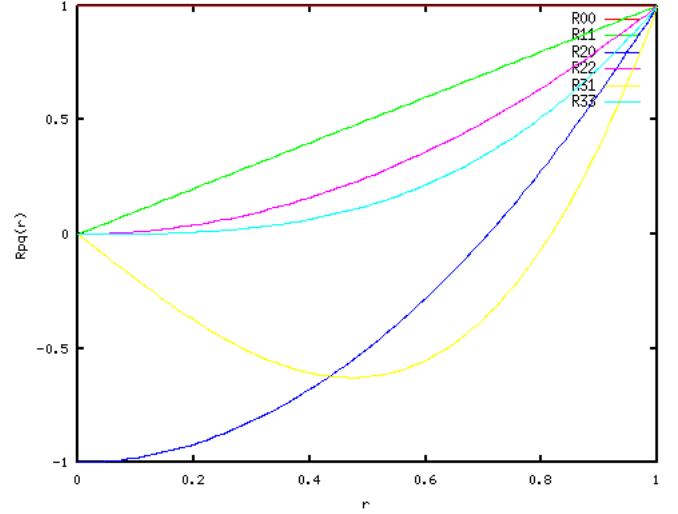


Fig. 2. Zernike radial function

$$Z_{pq} = \frac{(p+1)}{\pi} \sum_y \sum_x R_{pq} \left(\sqrt{x^2 + y^2} \right) e^{-i \cdot q \cdot \arctan(y/x)} f(x, y)$$

The magnitude of the Zernike's moment, i.e. $|Z_{pq}|$ is a descriptor invariant to the image rotation.

For more theoretical background about the Zernike moments refer to the following works [8], [9], [12], [20].

B. Pseudo Zernike Moments

Pseudo Zernike moments have been proposed as an improvement to the Zernike moments, where the former have been proven to have a superior feature representation capabilities and they are more robust in the presence of image quantization and error (see [21]). The differences with the Zernike moments are: The restriction that $p - |q|$ is even is eliminated and the radial function (figure 3) is computed as follows:

$$R_{pq}(r) = \sum_{s=0}^{p-|q|} (-1)^s \cdot \frac{(2p+1-s)! \cdot r^{p-s}}{s! \cdot (p-|q|-s)! \cdot (p+|q|+1-s)!} \quad (1)$$

The pseudo Zernike moments provide a higher number of linear independent polynomials of order $\leq p$, i.e., it contains $(p+1)^2$ polynomials whereas the Zernike polynomial contains only $\frac{1}{2}(p+1)(p+2)$. One disadvantage of the pseudo Zernike moments is their greater computational cost due to the increased number of terms per order [22].

C. Support Vector Machine

The Support Vector Machine (SVM) is a well-known and widely used technique for classification and regression problems existing in several fields [20]. For classification purposes, the SVM works as a supervised learning technique that attempts to construct a hyperplane that separate with maximum

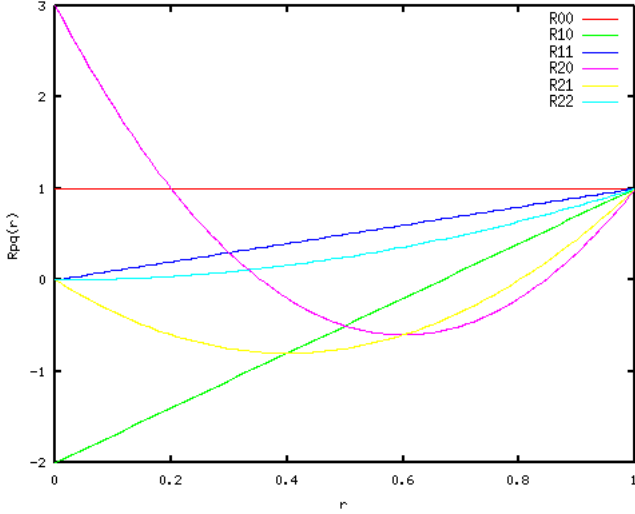


Fig. 3. Pseudo Zernike radial function

margin the data of two classes (a problem with more than 2 classes can also be reduced to a problem of two classes [23]). This hyperplane is obtained as a result of the following optimization problem:

$$\begin{aligned} \text{Minimize} \quad & Z(w, \xi) = \frac{1}{2} \|w\|^2 + \frac{C}{m} \sum_{i=1}^m \xi_i \\ \text{Subject to} \quad & y_i (\langle \phi(x_i), w \rangle + b) \geq 1 - \xi_i \quad (i = 1 \dots m) \\ & \xi_i \geq 0 \quad (i = 1 \dots m) \end{aligned}$$

where m is the number of training patterns, $\langle \cdot \rangle$ is the dot product, ϕ is an implicit mapping, y_i is the label class (± 1), x_i is the data point, ξ is the upper bound of error and C is the penalty value.

III. METHODOLOGY

1) *Pre-processing stage*: First, we need to segment the portion that correspond to the iris from the image of the eye. The procedure heuristically searches for a possible location of the pupil center by checking the neighborhood of each central pixel with low intensity. Afterwards, the correct location of the pupil center (x_p, y_p) is detected by geometrically circumscribing the pupil to the square where the method takes into account the intensity difference between the pupil and the iris (see figure 4 as an exemplification of these steps). After that, the iris inner boundary together with pupil radius r_p are obtained. Finally, we create a circle of radius R ($r_p < R$) concentric to the pupil as was proposed by [24]. The segmented portion of the iris corresponds to the region that covers from the pupil boundary up to the circle of radius R . This does not involve mayor problem, since it is known that the most important information of the iris is close to the pupil [25].

Most image processing algorithms work with images that can be mapped to a bidimensional matrix. For this reason we apply a normalization step to transform an image with an annulus shape to an square image data structure. To accomplish this task, we applied the polar transform in a similar way than the works of [3] and [4]:

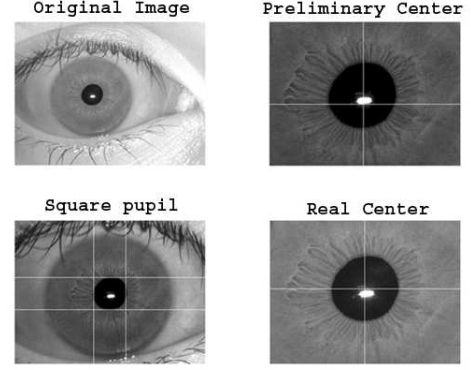


Fig. 4. Automatic localization of the pupil.

$$J(x, y) = IE(x_p + r(x) \cos(\theta(y)), y_p + r(x) \sin(\theta(y))) \quad (2)$$

where $J(x, y)$ is the normalized iris images and $IE(\cdot, \cdot)$ is the segmented iris image with a annulus shape, (x_p, y_p) is the center of the pupil, and, $r(x)$ and $\theta(y)$ are functions defined in equations (3) and (4) respectively.

$$r(x) = r_p + (x - 1) \Delta_r \quad \forall x \in \mathbb{N}, x \leq \frac{R - r_p}{\Delta_r} \quad (3)$$

$$\theta(y) = \begin{cases} \alpha_1 + (y - 1) \Delta_\theta, & \text{if } y \leq \frac{\alpha_s}{2 \Delta_\theta} \\ \alpha_2 + (y - 1) \Delta_\theta, & \text{if } y > \frac{\alpha_s}{2 \Delta_\theta} \end{cases} \quad \forall y \in \mathbb{N}, y \leq \frac{\alpha_s}{\Delta_\theta} \quad (4)$$

where r_p and R are the values of the radius of the pupil and the iris respectively, Δ_r is the interval of separation between pixels of the same radio (if $\Delta_r = 1$ means that there is no separation), Δ_θ is the interval of the angle separation, α_1 and α_2 are the starting end ending angles respectively, to scan and transform the image. α_s is the total angle covered by the full scan. The result of this transformation is exemplified in figure 5.

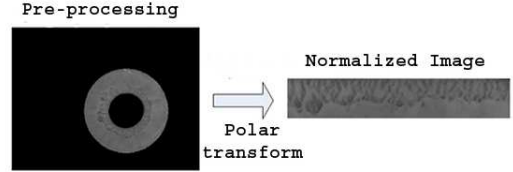


Fig. 5. Normalization process of the iris segment.

We decided to apply an scanning angle of 90 degrees for the left (from 135 degrees up to 225 degrees) and right (from -45 degrees up to 45 degrees) sections of the iris, and we do not consider the upper and lower parts of the iris due to the possible occlusions produced by eyelashes.

The normalized iris image has very low contrast and it could have a non-uniform brightness in different parts of the image

due to the light applied at the acquisition time. This makes the iris texture seem to be with less contrast than it really is. The contrast enhancement of the image is accomplished by means of a histogram equalization in order to use the full spectrum of gray levels, hence the textures are highlighted (see figure 6). Histogram equalization is easily obtained by resizing the gray intensities between 0 for the darker pixel and 255 for the whiter pixel, afterwards the values of all the pixels are replaced with their new intensity value. The new gray levels for each pixel are obtained with the following equation:

$$S^*(p) = \text{Round} \left(\frac{S(p) - S_{\min}}{255 - S_{\min}} \cdot 255 + 0.5 \right) \quad (5)$$

where $\text{Round}()$ is the operation of rounding to the nearest integer, $S(p)$ is the gray level value of the pixel p of the normalized image, S_{\min} is the smallest gray value of the normalized image and $S^*(p)$ is the new gray value of the pixel p of the enhanced image.

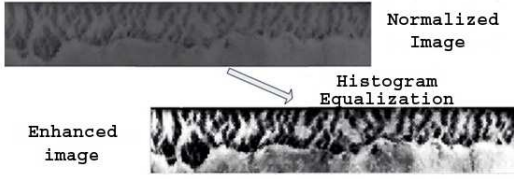


Fig. 6. Enhancement of the iris normalized image.

2) *Feature extraction*: In order to obtain the Zernike moment Z_{pq} , the coordinate system of each image was mapped into the unitary circle and centered in its centroid using the following transformation $x' = \frac{(x-cx)}{M}$ and $y' = \frac{(y-cy)}{M}$, where (x, y) are the original coordinates of the image, (cx, cy) is the centroid and $M = \max(\text{width}, \text{height})$. The Zernike moments were computed using this new coordinate system and considering only those points satisfying the condition: $(x')^2 + (y')^2 \leq 1$. Then feature vectors with different amount of moments were created, ordered from lower to higher order moments. The same steps were performed with pseudo Zernike.

3) *Classification*: The classification was made with the LibSVM library [26] with the tools provided by this library to split and scale data, and select the parameters of the kernel. The attributes of the data are scaled to the range $[-1, 1]$ in order to avoid dominating attributes with high values.

The kernel used was the radial basis function (RBF) $K(x_i, x_j) = \exp(-\gamma \|x_i - x_j\|^2)$, $\gamma > 0$. It is a nonlinear kernel that allows to handle the case when the relation between class labels and attributes are nonlinear. The RBF has two parameters: C and γ ; these parameters were tuned using the svm-grid tool provided by the libsvm library using a 5-fold cross-validation in order to prevent the overfitting problem.

IV. EXPERIMENTAL DETAILS AND SIMULATION RESULTS

For our experiments, we used the database obtained from the University of Bath repository [18]. The data set consists

of 1000 images corresponding to 25 different subjects with 20 images for each eye. The images are in grayscale with an original size of 1280 by 960 pixels, but we reduced down to 800 by 600 pixels.

Due to the intrinsic difference in the patterns of the iris of the left and right eye of each person [27], we considered each eye as a different class, so the total number of classes sum up to 50.

For the experiments we considered 939 images of the database since the remaining 61 were not properly pre-processed. However the distribution of images per subject is fairly uniform with a minimum of 13 images per class. The data was split into five sets of 188 samples each, but the last one that contains only 187 samples. Four of this groups were used for training and one for testing by following the 5-Folds cross-validation approach.

The Zernike and pseudo Zernike moments were extracted from the iriscode image under the following configuration. The quantity of moments used to describe the iris pattern were 10, 30, 50, 70, 90, 110 and 130, starting from the lower order moments (excluding the zero order) and increasing in order and repetitions up to the user-defined number of moments. The maximum order/repetition used was 21/19 for Zernike moments and 15/10 for the pseudo Zernike moments. The experiments were identically conducted for Zernike and pseudo Zernike obtaining the following results:

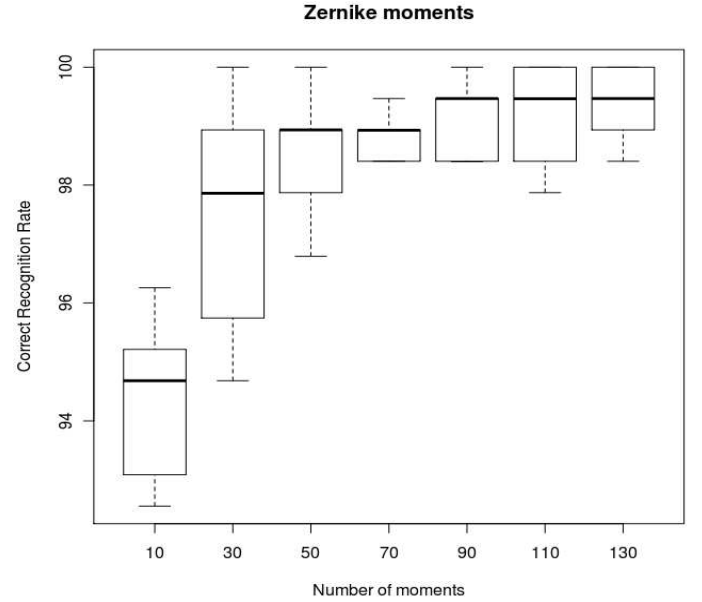


Fig. 7. Correct recognition rate at each fold with respect to the number of Zernike moments.

Figures 7 and 8 show the boxplot of the performance of the Zernike and Pseudo-Zernike moments respectively, where the performance were evaluated with the correct recognition rate. Figure 9 comparatively shows the performance of both descriptors, where we can easily notice that the Pseudo-Zernike moments outperforms the descriptive power of its classical counterpart. The best average correct recognition rate

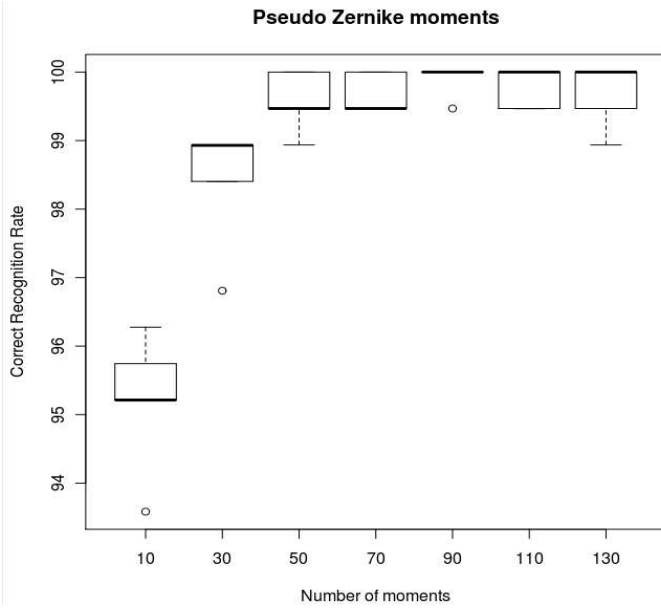


Fig. 8. Correct recognition rate at each fold with respect to the number of pseudo Zernike moments.

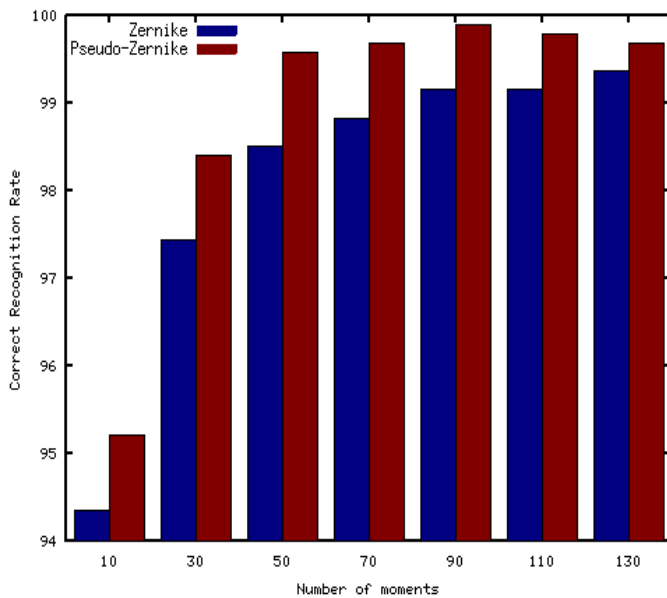


Fig. 9. Average correct recognition rate of the 5-folds accuracy of Zernike and pseudo Zernike moments.

obtained with Zernike Moments was 99.36% by using 130 moments while for pseudo Zernike was 99.89% by using 90 moments. The pseudo Zernike moments achieve better results than the Zernike moments probably due to the improved radio basis function R_{pq} .

V. CONCLUDING REMARKS

The present work has empirically demonstrated the good performance of Zernike and pseudo Zernike moments as object descriptor and the strong classifier that can be constructed

when the Zernike moments are combined with SVM. The pseudo Zernike moments show a better performance than the Zernike moments using the proposed methodology.

Future work involve the selection of the most representative moments in order to represent the object with a small but discriminant set of features. In addition, we will perform a multi-scale study on the image of the iris to reduce the computational complexity. Moreover, we will increase the number of classes in the database with the aim of increasing the difficulty of the identification task.

REFERENCES

- [1] J. Daugman, "High confidence visual recognition of persons by a test of statistical independence," *IEEE Transactions on Pattern Analysis and Machine Intelligence*, vol. 15, no. 11, pp. 1148–1161, 1993.
- [2] R. Wildes, "Iris recognition: An emerging biometric technology," *Proceedings of the IEEE*, vol. 85, no. 9, pp. 1348–1363, 1997.
- [3] J. Daugman, "How iris recognition works," *IEEE Trans. Circuits Syst. Video Techn.*, vol. 14, no. 1, pp. 21–30, 2004.
- [4] R. Sánchez-Reillo and C. Sánchez-Ávila, "Iris recognition with low template size," in *AVBPA*, ser. Lecture Notes in Computer Science, J. Bigün and F. Smeraldi, Eds., vol. 2091. Springer, 2001, pp. 324–329.
- [5] S. Cho and J. Kim, "Iris recognition using LVQ neural network," in *ISNN (2)*, ser. Lecture Notes in Computer Science, J. Wang, Z. Yi, J. M. Zurada, B.-L. Lu, and H. Yin, Eds., vol. 3972. Springer, 2006, pp. 26–33.
- [6] V.-E. Neagoe, "New self-organizing maps with non-conventional metrics and their applications for iris recognition and automatic translation," in *ICCOMP'07: Proceedings of the 11th WSEAS International Conference on Computers*. Stevens Point, Wisconsin, USA: World Scientific and Engineering Academy and Society (WSEAS), 2007, pp. 145–151.
- [7] G. Papakostas, Y. Boutalis, C. Papaodysseus, and D. Fragoulis, "Numerical error analysis in Zernike moments computation," *Image Vision Computing*, vol. 24, no. 9, pp. 960–969, 2006.
- [8] A. Khotanzad and Y. Hong, "Invariant image recognition by Zernike moments," *IEEE Trans. Pattern Analysis and Machine Intelligence*, vol. 12, pp. 489–497, May 1990.
- [9] E. Arvacheh and H. Tizhoosh, "Pattern analysis using Zernike moments," in *Instrumentation and Measurement Technology Conference, 2005. IMTC 2005. Proceedings of the IEEE*, vol. 2, may 2005, pp. 1574 – 1578.
- [10] C. Lu and Z. Lu, "Zernike moment invariants based iris recognition," in *SINOBIOMETRICS*, ser. Lecture Notes in Computer Science, S. Li, J. Lai, T. Tan, G. Feng, and Y. Wang, Eds., vol. 3338. Springer, 2004, pp. 554–561.
- [11] C. Deepika, A. Kandaswamy, C. Vimal, and B. Sathish, "Invariant feature extraction from fingerprint biometric using pseudo Zernike moments," *International Journal of Computer Communication and Information System (IJCCIS)*, vol. 2, pp. 104–108, 2010.
- [12] E. Kintner, "On the mathematical properties of the zernike polynomials," *Optica Acta*, vol. 23, no. 8, pp. 679–680, 1976.
- [13] S. Hwang and W. Kim, "A novel approach to the fast computation of zernike moments," *Pattern Recognition*, vol. 39, pp. 2065–2076, 2006.
- [14] C.-W. Chong, P. Raveendran, and R. Mukundan, "An efficient algorithm for fast computation of pseudo-zernike moments," *IJPRAI*, vol. 17, no. 6, pp. 1011–1023, 2003.
- [15] J. Haddadnia, M. Ahmadi, and K. Faez, "An efficient feature extraction method with pseudo-zernike moment in rbf neural network-based human face recognition system," *EURASIP J. Appl. Signal Process.*, vol. 2003, pp. 890–901, January 2003. [Online]. Available: <http://dx.doi.org/10.1155/S1110865703305128>
- [16] A. Nabatchian, I. Makaremi, E. Abdel-Raheem, and M. Ahmadi, "Pseudo-zernike moment invariants for recognition of faces using different classifiers in feret database," in *Proceedings of the 2008 Third International Conference on Convergence and Hybrid Information Technology - Volume 01*. Washington, DC, USA: IEEE Computer Society, 2008, pp. 933–936. [Online]. Available: <http://dl.acm.org/citation.cfm?id=1471603.1471723>
- [17] A. Pokhriyal and S. Lehri, "A new method of fingerprint authentication using 2d wavelets," *Theoretical and Applied Information Technology*, vol. 13, no. 2, 2010.

- [18] D. Monro, "Bath University iris database," University of Bath, Bath, School of Electronic and Electrical Engineering, 2008, <http://www.bath.ac.uk/elec-eng/research/sipgl>.
- [19] F. Zernike, "Diffraction theory of the cut procedure and its improved form, the phase contrast method," *Physica*, vol. 1, pp. 689–704, 1934.
- [20] V. Vapnik, *The Nature of Statistical Learning Theory*. Information Science and Statistics: Springer, 1999.
- [21] C. Teh and R. Chin, "On image analysis by the method of moments," *IEEE Trans. on Pattern Analysis and Machine Intelligence*, vol. 10, no. 4, pp. 496–513, 1988.
- [22] K. Marsolo, S. Parthasarathy, M. Twa, and M. A. Bullimore, "Classification of biomedical data through model-based spatial averaging," in *Proceedings of the Fifth IEEE Symposium on Bioinformatics and Bioengineering*, ser. BIBE '05. Washington, DC, USA: IEEE Computer Society, 2005, pp. 49–56. [Online]. Available: <http://dx.doi.org/10.1109/BIBE.2005.16>
- [23] C.-W. Hsu and C.-J. Lin, "A comparison of methods for multi-class support vector machines," *IEEE Transactions on Neural Networks*, vol. 13, no. 2, pp. 415–425, 2002.
- [24] B. Ganeshan, D. Theckedath, R. Young, and C. Chatwin, "Biometric iris recognition system using a fast and robust iris localization and alignment procedure," in *Optics and Lasers in Engineering*, vol. 44, 2006, pp. 1–24.
- [25] K. Rogers, *The eye: the physiology of human perception*, ser. First edition. New York: Britannica Educational Publishing in association with Rosen Education Service, 2010.
- [26] C. Chang and C. Lin, "LIBSVM: A library for support vector machines," *ACM Transactions on Intelligent Systems and Technology*, vol. 2, pp. 27:1–27:27, 2011, software available at <http://www.csie.ntu.edu.tw/~cjlin/libsvm>.
- [27] A. R. A. Jain and P. Flynn, *Handbook of Biometrics*. Springer-Verlag, 2008.